IEEE Access
Multidisciplinary | Rapid Review | Open Access Journal

Received June 18, 2019, accepted July 8, 2019, date of publication July 17, 2019, date of current version August 5, 2019.

Digital Object Identifier 10.1109/ACCESS.2019.2929525

Theoretical Analysis of REM-Based Handover Algorithm for Heterogeneous Networks

CRISTO SUAREZ-RODRIGUEZ, (Student Member, IEEE), YING HE, (Member, IEEE), AND ERYK DUTKIEWICZ, (Senior Member, IEEE)

Global Big Data Technology Center, University of Technology Sydney, Ultimo, NSW 2007, Australia

Corresponding author: Cristo Suarez-Rodriguez (cristo.suarez-rodriguez@student.uts.edu.au)

ABSTRACT Handover has been a widely studied topic since the beginning of the mobile communications era, but with the advent of another generation, it is worth seeing it with fresh eyes. Data traffic is expected to keep growing as new use cases will coexist under the same umbrella, e.g., vehicle-to-vehicle or massive-machine-type communications. Heterogeneous networks will give way to multi-tiered networks, and mobility management will become challenging once again. Under the current approach, based uniquely on measurements, the number of handovers will soar, so will the signaling. We propose a handover algorithm that employs multidimensional radio-cognitive databases, namely radio environment maps, to predict the best network connection according to the user's trajectory. Radio environment maps have been extensively used in spectrum-sharing scenarios, and recently, some advances in other areas have been supported by them, such as coverage deployment or interference management. We also present a geometric model that translates the 3GPP specifications into geometry and introduce a new framework that can give useful insights into our proposed technique's performance. We validate our framework through Monte Carlo simulations, and the results show that a drastic reduction of at least 10% in the ping-pong handovers can be achieved, thus reducing the signaling needed.

INDEX TERMS Handover, handover failure, heterogeneous networks, ping-pong handover, radio environment map.

I. INTRODUCTION

Network densification has come to stay. Year after year the demand for data-intensive applications has steadily increased as well as the deployment of small cells and Wi-Fi hotspots to keep up with the current trend and to take a share of users' traffic [1]. The addition of small cells underlying the coverage of macrocells to improve the capacity per unit area in the most crowded urban areas or at cell edges was included in the Long-Term-Evolution (LTE) standard releases. Moreover, ultra-densification has been envisioned to play a key role in 5G, where network heterogeneity will be a more prominent feature with the new 5G standard along with legacy standards and multi radio-access technologies [2].

The inclusion of small cells helps to offload the loaded macro tier by shrinking its coverage area, although some problems arise. Mobility users face a higher cross-tier handover (HO) rate due to smaller sojourn times, impacting negatively on their quality of service (QoS) as a consequence of the signaling needed. Too many HOs are unnecessary if users are not connected long enough to their serving cell (ping-pong effect, PP), while too few will lead to a signal loss (handover failure, HF). The nature of the problem is combinatorial as a result of the existence of multiple handover-related parameters such as the time-to-trigger (TTT) or the handover hysteresis margin (HHM) [3].

As a result, the 5G New Radio (5G NR) specification has added a feature called conditional HO (CHO) [4], where the baseline LTE-HO procedure has been split into two separate events. In the LTE-HO procedure, once the conditions for an HO has been met, it automatically follows an HO execution, i.e. a user equipment (UE) starts the random access procedure in the target cell. In the CHO procedure, once the conditions for an HO has been met, it triggers a CHO preparation without a CHO execution. The execution is left to the UE to decide an optimal time or in case of an imminent radio link failure (RLF) [5]. On the one hand, the CHO preparation can be done in advance, reducing the delay when camping on the new cell,

The associate editor coordinating the review of this manuscript and approving it for publication was Maurice J. Khabbaz.

thus virtually reducing potential HFs or RLFs to zero [6]. On the other hand, CHO requires having an updated list of candidate cells where the CHO preparation has been done, even though at most only one potential HO will be executed, increasing signaling.

In this work, we want to evaluate and analyze the impact of the location errors on a novel HO algorithm compatible with 5G NR, supported by radio environment maps (REM), namely REM-Based HO (REM-HO). REMs have also been extensively used for spectrum sharing in television white spaces (TVWS) [7], and their integration within an LTE network has been discussed in [8]. A REM has been proposed as a database for spatial spectrum sharing [9], which stores the average received signal strength (RSS) spatially. Moreover, the authors show that the estimation error of the Kriging-based REM follows a log-normal distribution, where the predicted RSS values are below 8 dB root-mean-square error (RMSE). In [10], we employ REMs in the HO decision making to help us estimating the channel conditions in the short term (seconds scale) knowing the UE's location and trajectory to avoid PP HOs. Nonetheless, only simulation results are provided, i.e. we do not present closed-form expressions, and the proposed technique relies on static parameters. In [11], we show preliminary theoretical results applied to a simple network comprised of only one macrocell and one picocell, disregarding location errors altogether. Nonetheless, introducing geolocation awareness also imposes the challenge of dealing with location errors, and hence, HFs might also be frequent.

In this paper, we further develop our theoretical framework to accommodate a whole network and take into account the location uncertainty. Thus the contributions of this paper can be summarized as below:

- An analytical framework for our proposed REM-HO algorithm that extends our work in [10], [11] is developed. Based on the specifications for LTE and 5G-NR ready, we derive the probabilities of no handover, handover failure, and ping-pong handover in a two-tier heterogeneous network as functions of the mobility parameters and geolocation information.
- We carry out an optimization problem to fine tune our algorithm and validate our theoretical analysis through Monte Carlo simulations. To provide insight into the impact of location errors in our proposed technique, we also compare it against the conventional LTE-HO algorithm. From the results, we show that our algorithm can avoid most of the PP HOs between tiers for user speeds up to 120 km/h. However, location errors penalize in terms of HF the most due to the similar range between the errors and the distance travelled by the users during the HO process.

The paper is organized as follows. Section II introduces relevant works in the literature, Section III presents an overview of the system model employed. Section IV explains the REM-HO algorithm and presents the set of equations used to describe the proposed algorithm. In Section V, we validate our theoretical approach by numerical evaluation and discuss how some relevant parameters affect the performance of our proposed algorithm. We also show a performance comparison with the LTE-HO algorithm. Finally, Section VI states the main findings of this work and gives a summary.

II. RELATED WORK

Mobility management (MM) has been extensively studied in both industry and academia [3], [12]–[15]. In [3], the 3rd Generation Partnership Project (3GPP) established a series of simulation guidelines to assess improvements in seamless and robust mobility across heterogeneous networks (HetNets). Lopez-Perez *et al.* [12] studied the effect of the range expansion bias on picocells' footprints and derived their boundaries as concentric circular regions. In [13], the same authors characterized the relation between HF and PP rates in a 3GPP HetNet scenario in closed-form expressions assuming that UEs follow linear trajectories. Vasudeva *et al.* [14] further extended this model to deal with fading, taking into account the L1 and L3 filtering. After collecting data from a 3GPP-compliant simulator, they concluded that fading could be incorporated in the formulation as a random variable on top of the measurement period. Guidolin *et al.* [15] proposed an original Markov-based framework that exploits some parameters (e.g. the path-loss coefficients, the user speed, and the cell load factors among others) to derive an optimal TTT context-dependent parameter from limiting the number of HOs and also the signaling between the cells. They showed an improvement in the users capacity against fixed-TTT policies.

An extensive body of work has been developed in recent years employing stochastic geometry as a way to provide a tractable model to evaluate a wide range of techniques in cellular communications [16]–[20]. Both Dhillon *et al.* [16] and Jo *et al.* [17] delivered seminal papers that laid the foundation of stochastic geometry for multi-tier networks. The main difference between them is the cell association criteria: the former uses the instantaneous power while the latter used the average power, which is closer to the actual behavior of LTE and 5G-NR. Xu *et al.* [18] bridged previous works with stochastic geometry. They showed that the picocell coverage area is a circle and extended this result to a whole network employing the void probability of a Poisson point process. Then, the cross-tier HO rate is analyzed in a simplified model with the random waypoint mobility model. Similarly, the authors in [19] characterized the HO rate in a multi-tier HetNet with an arbitrary mobility model. An extension to this work can be found in [20], where the user data rate is also expressed in closed form.

Focusing on HO techniques, Arshad *et al.* [21] proposed a velocity-aware HO management scheme that skips HOs to some base stations (BSs) along the user trajectory. It skips the best BS available; however, BS cooperation is allowed to improve the average capacity. Several strategies to select which BS to skip are presented, and results show up to 77% more rate gains for user speed ranging from 80 km/h to

200 km/h when compared to the conventional best-BS HO scheme. Same authors expanded their work in [22] by adding location-awareness, where HOs are skipped if the distance between the user trajectory and the target BS exceeds a predefined threshold. They noted that errors in the trajectory estimation might reduce the performance of their proposed strategies. However, all these techniques employ double the bandwidth to provide their claimed gains due to the cooperative transmission scheme they are based on.

In [23], Becvar and Mach propose a novel HO decision algorithm based on the estimation of throughput gain in case of handing over to femtocells. Coordination between macrocells and femtocells via backbone is exploited to mitigate redundant HOs. The increase in throughput is derived from an extrapolation of the previous measurements performed by UEs; then the HO is only executed if the gain is above a predefined threshold. However, their method has two significant drawbacks: first, the estimated gain relies on the prediction of the sojourn time within the cell, which in turn reduces the applicability of the algorithm to hand-in only; and second, the method is aimed to pedestrians. On a similar note, Xenakis *et al.* [24] introduce an HO decision algorithm for LTE that takes into account both the interference at the UE side and its battery life designed for indoor use. They optimize two HHMs: the first one skips cells that might compromise service continuity, i.e. drops, whereas the second one identifies the cell with the minimum required UE transmit power. The method exchanges the interference at the UE side for the cell side and increases the utilization of the femtocells, so does the handover probability. In our approach, REMs can successfully help obtain a better prediction in terms of RSS, while the sojourn time is not relevant. Also, we cannot neglect the existence of small cells in high-mobility scenarios such as light rail in the business districts of big cities.

Chen *et al.* [25] present a framework of HO decision in LTE networks under a high-speed mobility scenario, i.e. up to 500 km/h. They investigate a Location-Based HO decision algorithm that makes use of the information about the relative location between the train and the cells down the tracks. By analyzing the speed information sensed by the tachometer, the UE sends a measurement report of its current distance and velocity to the serving cell. Although the framework could be easily adapted to low-speed environments, the algorithm only considers a homogeneous network, where the cell edges correspond to the midpoint between cells. Our proposed algorithm capitalizes on the geolocation of the UEs across the network, widely available in modern hand-held devices, and adaptively adjusts the prediction depending on the nature of the target cell. Thus it is not restricted to macro-only or pico-only networks.

A common criticism in the literature is the lack of tractability [26], most of the works above in HO decision algorithms present their results in the form of performance analysis, which may be insufficient to derive useful insights and provide mathematical results for the expected performance. For example, in [27], Kuang *et al.* study the HF and PP HO rates

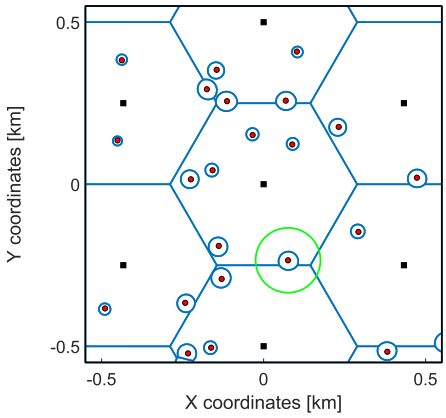

FIGURE 1. Coverage regions (blue lines) in a two-tier cellular network. Macrocells (black squares) are in a hexagonal grid with ISD = 500 m and picocells (red circles) are uniformly deployed. Users bounce within the green circle with radius = 100 m as per 3GPP specifications [3].

based on a HetNet field-trial activity. Then the measured data are used as inputs to their simulation models. Despite its relevance, from a theoretical standpoint is difficult to extend their conclusions to any other given network. K. da Costa Silva *et al.* [28] propose a fuzzy logic-based HO scheme exploiting the user's velocity and its radio channel quality to adapt an HHM in a self-organizing manner. This dynamic adaptation minimizes the number of redundant HOs and HFs. However, the intervals and granularity of the input parameters - namely speed, channel quality, and received power - are based solely on the 3GPP specifications [29], meaning that it only adapts for a very narrow range of networks. There is no method to adapt their definitions to a network that might not experience the range of studied values.

The novelty of our proposed algorithm is mostly two-fold: first, we provide analytical results that are verified by simulations, so they can be adapted to a wide range of HetNets scenarios, where different parameters come into play; and second, we tune our algorithm to reflect the current combination of UE's location and speed, in fact in an adaptive manner.

III. SYSTEM MODEL

In this section, we provide a model so that we can describe the handover regions analytically. We consider the long-term cell association based solely on the path loss (fading is averaged out [17], [18]). Moreover, we introduce the location error model focusing on the Global Positioning System (GPS) [30]. Hereafter, we describe the main models needed for a clear understanding of our proposed approach.

A. GEOMETRIC MODEL

We consider a two-tier HetNet comprised of a macrocell tier (tier m) and a picocell tier (tier p). We assume that both tiers operate on the same spectrum. Following the 3GPP specifications [3] (see Table 1), the macrocell tier is arranged in a hexagonal grid whereas the picocell tier is uniformly deployed within the coverage areas of macrocell BSs as shown in Fig. 1. Considering that the BSs in the same tier

$i = \{m, p\}$ have the same transmit power $P_{t,i}$ and antenna gain G_i, the received signal strength $P_{r,i}$ at a distance d_i can be expressed as the following:

$$P_{r,i} = P_{t,i} G_i K_i d_i^{-\gamma_i}, \tag{1}$$

where K_i is the attenuation at the reference distance and γ_i is the path-loss exponent that takes into account the specific characteristics of the propagation environment, i.e. the frequency, the antenna height, among others. A macrocell UE will start the HO procedure to the picocell when $P_{r,m}$ drops below $P_{r,p}$ plus a certain HHM α, namely A3 event (a neighbor becomes offset better than the server [31, Ch. 17]):

$$P_{r,m} < P_{r,p} + \alpha \text{ [dBm]}. \tag{2}$$

In this scenario, under the assumption that the macrocell has a transmit power significantly higher than the picocell (16–22 dB difference [18]), the handover region converges to a circle [12, Theorem 1]. Without loss of generality, we assume that a macrocell BS is at the origin, and a picocell BS is at location $\mathbf{x_p} = (0, d)$, then the picocell coverage area is a circle with the center $\mathbf{x_c}$ and the radius R_c given as follows:

$$\mathbf{x_c} = \left(0, \frac{\mathcal{Z}}{\mathcal{Z}-1} d\right), \quad \text{and} \tag{3}$$

$$R_c = \frac{\sqrt{\mathcal{Z}}}{\mathcal{Z}-1} d, \tag{4}$$

where $\mathcal{Z} = \left(\frac{\alpha P_{t,m} G_m K_m}{P_{t,p} G_p K_p}\right)^{2/\gamma_p}$. For simplicity, we assume that $\gamma_m = \gamma_p$. Similar expressions can be obtained for the general case when $\gamma_m \neq \gamma_p$ as presented in [13], [18], but comes at the expense of more involved expressions.

Similarly, a handover failure is declared when the macrocell UE's wideband signal-to-noise-plus-interference ratio (SINR) is below a threshold $Q_{\text{out}} = -8$ dB. Hence we can define the macrocell handover failure circle with the center $\mathbf{x_f}$ and the radius R_f given as:

$$\mathbf{x_f} = \left(0, \frac{\mathcal{Z}_f}{\mathcal{Z}_f - 1} d\right), \quad \text{and} \tag{5}$$

$$R_f = \frac{\sqrt{\mathcal{Z}_f}}{\mathcal{Z}_f - 1} d, \tag{6}$$

where $\mathcal{Z}_f = \mathcal{Z} Q_{\text{out}}^{-2/\gamma_p}$. In the case of homogeneous networks or horizontal HO, where the BSs in the same tier $i = \{m, p\}$ have the same transmit power $P_{t,i}$ and antenna gain G_i, then $\mathcal{Z} = \alpha^{2/\gamma}$, which means that the HHM is the only parameter that affects the shape of the circle. Depending on the value of α, we can have:

1) $\alpha \neq 0$ dB $\rightarrow \{\mathcal{Z}, \mathcal{Z}_f\} \neq 1$, then (3)–(6) represent circles, and our algorithm can be normally applied.
2) $\alpha = 0$ dB $\rightarrow \{\mathcal{Z}, \mathcal{Z}_f\} = 1$, then (4) represents a circle with infinite radius, i.e. a straight line. To be precise, it becomes the bisector of the segment that links two given BSs. For example, in Fig. 1, the hexagonal grid is the superposition of different segment bisectors among the macrocells. The macrocell handover failure circle would remain. Our algorithm could still be applied but it would not give any significant advantage over LTE in terms of PP HO since there is no coverage circle to avoid.

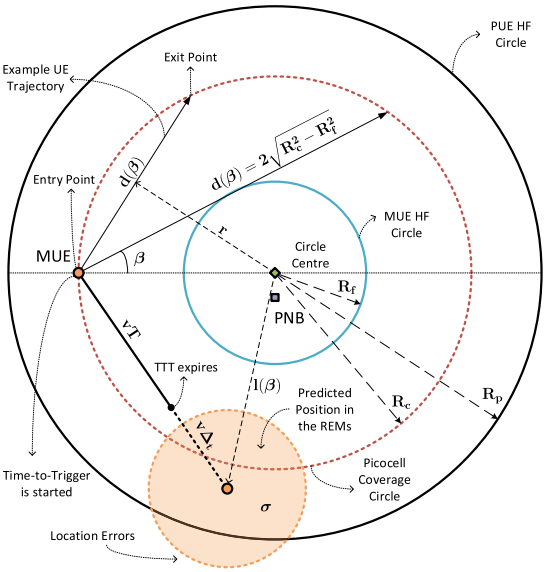

FIGURE 2. Models for picocell coverage area and macrocell and picocell HF areas.

B. MOBILITY MODEL

We assume that the macrocell UEs move with a constant speed v on an arbitrary trajectory within a concentric circle around a picocell (green circle in Fig. 1) whose radius is larger than the radius of the picocell coverage circle. The starting position is chosen randomly on the circumference of the circle; then the UE follows a random linear trajectory towards the picocell until it becomes a chord of the circle, i.e. a straight line whose endpoints both lie on the circumference. Its arrival angle to the picocell coverage area β in Fig. 2 is uniformly distributed in $\left[-\frac{\pi}{2}, \frac{\pi}{2}\right]$. Let $d(\beta) = 2\, R_c \cos(\beta)$ denote the length of the chord formed by the entry and exit points of a UE crossing the picocell coverage area, and r be the distance from the center of the picocell area to the chord $d(\beta)$. The probability density function (PDF) of r follows [13]:

$$f(r) = \frac{2}{\pi \sqrt{R_c^2 - r^2}}, \quad 0 \leq r \leq R_c. \tag{7}$$

Therefore, the probability of the chord being between two given lengths d_1 and d_2, with $d_1 < d_2$ is given by:

$$\mathbb{P}(d_1 < d(\beta) < d_2) = \frac{2}{\pi} \arctan\left(\frac{r}{\sqrt{R_c^2 - r^2}}\right) \Bigg|_{\sqrt{R_c^2 - d_1^2/4}}^{\sqrt{R_c^2 - d_2^2/4}}. \tag{8}$$

When UEs send measurement reports to their serving macrocell to perform an HO to the picocell [3], we assume that they also send back their location and velocity information. In this context, the UE's position provided by either

a Global Navigation Satellite System (GNSS) or a cellular network-assisted technique is altered by location errors. Nowadays, the most universally available system is GPS. Therefore our analysis considers it as a baseline. The GPS error model can be seen as a bivariate normal (Gaussian) distribution $\boldsymbol{\varepsilon} \sim \mathcal{N}_2(0, \boldsymbol{\Sigma})$, where $\boldsymbol{\varepsilon} = (x, y)$ is a random vector which describes the location errors and the positive-definite covariance matrix $\boldsymbol{\Sigma}$ given by

$$\boldsymbol{\Sigma} = \begin{pmatrix} \sigma_X^2 & \rho\sigma_X\sigma_Y \\ \rho\sigma_Y\sigma_X & \sigma_Y^2 \end{pmatrix}, \tag{9}$$

where σ_X and σ_Y represent the standard deviations of the errors at the North-South and the East-West directions, and ρ is the correlation factor between them [32]. For simplicity, we consider them to be independent in both the x and y directions and equal, i.e. $\rho = 0$ and $\sigma_X = \sigma_Y = \sigma$. Hence, the distance from the center of the picocell area to the reported location by the UE follows a Rice distribution $\kappa \sim \text{Rice}(\nu, \sigma)$, where ν denotes the true position of the UE. The cumulative distribution function (CDF) of κ is given as:

$$\mathbb{P}(\kappa < K) = 1 - Q_1\left(\frac{\nu}{\sigma}, \frac{K}{\sigma}\right), \tag{10}$$

where Q_1 is the Marcum Q-function [33]. Finally, GPS errors are also temporally and spatially autocorrelated, meaning that two consecutive position samples taken close in space and in time have similar errors, thus cancelling out when calculating averages [32]. The probabilities of no handover (NHO), handover failure (HF) and ping-pong handover (PP) will be derived based on (8) and (10).

IV. REM-BASED HANDOVER ALGORITHM

Once we have described the different models needed, we are in a position to introduce our proposed algorithm (Algorithm 1). We propose a REM-based HO algorithm aimed to reduce the number of ping-pong HOs without compromising the number of HFs. A REM is a spectrum database that stores the spatial distribution of the average RSS per cell [34]. Exploiting the stored RSS values and geolocation, we can pre-emptively classify an HO as worth doing according to the current UE's location. Since we could flag all the triggered HOs as unnecessary, we have to take the risk of possible HFs (drops) as well. Note that Algorithm 1 is written from the macrocell's point of view. From the picocell's perspective, we default to the standard LTE-HO algorithm.

When the user arrives at the border between the two cells, it starts a timer called Time-To-Trigger (TTT) of duration T [29]. Once the TTT expires[1] (see line 3 in Algorithm 1), our proposed algorithm predicts the user's position in a timespan Δ_t (line 8). This predicted point is then introduced in the macrocell and picocell REMs (each BS has one) to get the stored RSS values. Since our model only considers path loss, the handover region where the picocell RSS is higher than the macrocell RSS is exactly the circle defined in (3–4).

[1] We disregard the handover preparation and execution times [3].

Algorithm 1 REM-Based Handover Algorithm

1: **procedure** UE REM-HO($P_{r,m}$, $P_{r,p}$, α, T)
2: **if** $P_{r,m} + \alpha < P_{r,p}$ for T **then**
3: UE sends a measurement report with the user's location $\mathbf{x_u} = (x_u, y_u) + \varepsilon$, and velocity $\mathbf{v} = (v_x, v_y)$.
4: **end if**
5: **end procedure**

6: **procedure** BS REM-HO($\mathbf{x_u}$, $\mathbf{v}$, Δ_t, REM$_m$, REM$_p$)
7: **if** Measurement report received **then**
8: Predict the user's position in Δ_t. $\mathbf{x_p} = \mathbf{x_u} + \mathbf{v} \cdot \Delta_t$
9: **if** REM$_p(\mathbf{x_p})$ > REM$_m(\mathbf{x_p})$ **then**
10: BS sends the handover command back to the UE.
11: **end if**
12: **end if**
13: **end procedure**

Therefore, our policy allows the UE to hand over to the picocell only if the predicted point lies within the circle (lines 9–10). Otherwise, it will remain connected to the macrocell.

Nonetheless, an HF is declared if the UE's SINR is below Q_{out}, i.e. its trajectory intersects the HF circle. In the following, we derive the probabilities of NHO, HF for both macrocell and picocell UEs, and PP HOs. Such probabilities are conditioned on the distance between the macrocell and the picocell, which is uniformly distributed in an annulus with major and minor radii denoted by $r_{\max}$ and $r_{\min}$ [35]. In order to obtain the probabilities for the whole network, the probabilities must be weighted by the following PDF [36]:

$$f(x) = \frac{2\,(x - r_{\min})}{(r_{\max} - r_{\min})^2}, \quad r_{\min} \le x \le r_{\max}. \tag{11}$$

A. PROBABILITY OF NO HANDOVER

The probability of NHO represents the probability of a user leaving the handover region before the TTT expires without having a handover failure, i.e. intersecting the macrocell HF circle, which means that the chord must be shorter than the tangential chord ($2\sqrt{R_c^2 - R_f^2}$ in Fig. 2). Based on the distance that a macrocell UE can go across during a TTT of duration T, vT, we can distinguish two different cases. If vT is longer than the tangential chord, regardless of the prediction, the probability of NHO becomes the probability of the chord being between $0 < d(\beta) < 2\sqrt{R_c^2 - R_f^2}$ (8) as shown in Fig. 3 in the case of v_1T_1. In case that vT is shorter, both the TTT and the prediction time determine if there will be an HO. There will not be any HO if either the TTT expires outside the HO region ($0 < d(\beta) < vT$) or the TTT does expire within the HO region, but the prediction is outside without suffering from an HF. In Fig. 3, we show the case of v_2T_2 where T_2 can be either just the TTT or the addition of the TTT

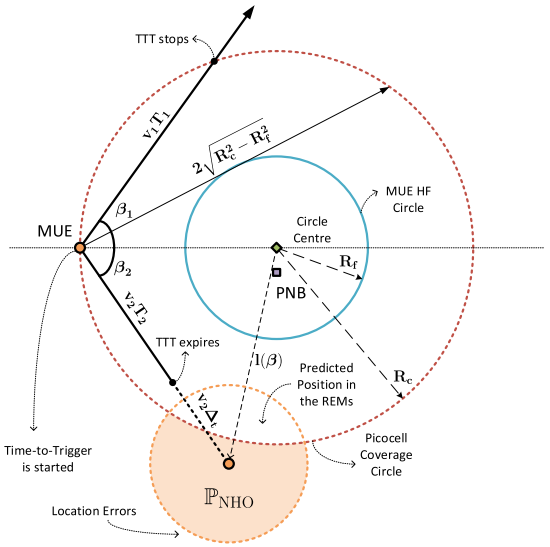

FIGURE 3. $\mathbb{P}_{\mathbf{NHO}}$.

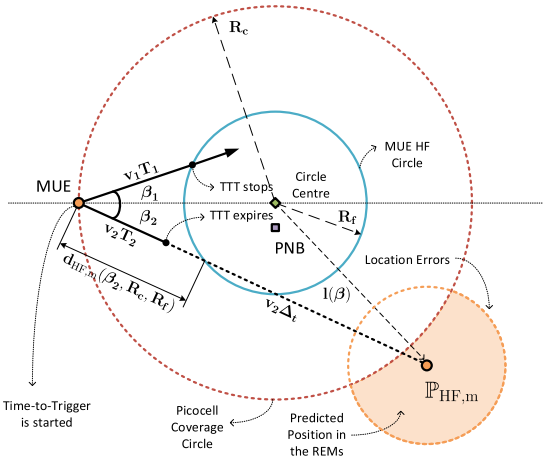

FIGURE 4. $\mathbb{P}_{\mathbf{HF,m}}$.

and the prediction time. Note that the prediction is affected by location errors. However, we can derive the center of the distribution as:

$$l(\beta) = \sqrt{v^2\,(T+\Delta_t)^2 + R_c^2 - 2v\,(T+\Delta_t)\,R_c\cos(\beta)}. \quad (12)$$

To avoid intersecting the macrocell HF area, the UE's trajectory must be between $\arcsin\left(R_f/R_c\right) < \beta \leq \arccos\left(vT/2R_c\right)$. Thus using (10), we can obtain

$$\mathbb{P}\left[l(\beta) > R_c\right] = \frac{2}{\pi}\int_{\arcsin(R_f/R_c)}^{\arccos(vT/2R_c)} Q_1\left(\frac{l(\beta)}{\sigma}, \frac{R_c}{\sigma}\right) \mathrm{d}\beta. \quad (13)$$

Taking everything into account, we can write (14), as shown at the bottom of this page.

B. PROBABILITY OF MACROCELL HANDOVER FAILURE

If the chord length is longer than the tangential one, it means the user's trajectory intersects the macrocell HF circle, and the possibility of handover failure is real. In our proposed algorithm, depending on where the TTT expires, two possible events might end up in a handover failure. The first one is the same as in LTE-A, in case the user reaches the macrocell HF circle before the TTT expires, an HF is declared as it can be seen in Fig. 4 with v_1T_1. The user reaches the macrocell HF circle if the distance during the TTT is longer than the distance between the starting point and the circle. It can be expressed as

$$vT \geq d_{\mathrm{HF,m}}(\beta, R_c, R_f), \quad (15)$$

where $d_{\mathrm{HF,m}}(\beta, R_c, R_f) = R_c\cos(\beta) - \sqrt{R_f^2 - R_c^2\sin^2(\beta)}$. For example, in Fig. 4 the distance is labeled as $d_{\mathrm{HF,m}}(\beta_2, R_c, R_f)$. Then, the probability of a UE reaching the macrocell HF circle is [13]:

$$\mathbb{P}\left[vT \geq d_{\mathrm{HF,m}}(\beta, R_c, R_f)\right] = \begin{cases} 1 & \text{if } vT \geq \sqrt{R_c^2 - R_f^2}, \\ \dfrac{\arccos\left[\frac{(vT)^2 + R_c^2 - R_f^2}{2vTR_c}\right]}{\arcsin\left(\frac{R_f}{R_c}\right)} & \text{if } R_c - R_F \leq vT \leq 2\sqrt{R_c^2 - R_f^2}, \\ 0 & \text{if } vT < R_c - R_f. \end{cases} \quad (16)$$

The second event that may lead to an HF is related to our proposed algorithm: even though the TTT expires before reaching the macrocell HF circle, if the prediction is not within the handover region, an HF will be declared since we skip that HO mistakenly only for trajectories between $0 \leq \beta \leq \arcsin\left(R_f/R_c\right)$. This can be observed in Fig. 4 with v_2T_2 and $v_2\Delta_t$. Similarly to the NHO probability, the center of the distribution is $l(\beta)$ in (12), but now we are interested in the UE's trajectories that intersect the macrocell HF area, i.e. $0 \leq \beta \leq \arcsin\left(R_f/R_c\right)$. Thus, the total probability of macrocell HF is given by (17), as shown at the bottom of this page.

$$\mathbb{P}_{\mathrm{NHO}} = \begin{cases} \mathbb{P}\left[d(\beta) < 2\sqrt{R_c^2 - R_f^2}\right] & \text{if } vT \geq 2\sqrt{R_c^2 - R_f^2}, \\ \mathbb{P}\left[d(\beta) < vT\right] + \mathbb{P}\left[l(\beta) > R_c\right] & \text{if } vT < 2\sqrt{R_c^2 - R_f^2},\ \arcsin\left(R_f/R_c\right) < \beta \leq \arccos\left(vT/2R_c\right). \end{cases} \quad (14)$$

$$\mathbb{P}_{\mathrm{HF,m}} = \mathbb{P}\left[d(\beta) > 2\sqrt{R_c^2 - R_f^2}\right] \cdot \mathbb{P}\left[vT \geq d_{\mathrm{HF,m}}(\beta, R_c, R_f)\right] + \mathbb{P}\left[l(\beta) > R_c\right] \cdot \mathbb{P}\left[vT < d_{\mathrm{HF,m}}(\beta, R_c, R_f)\right] \quad \text{if } 0 \leq \beta \leq \arcsin\left(R_f/R_c\right) \quad (17)$$

C. PROBABILITY OF PICOCELL HANDOVER FAILURE AND PING-PONG HANDOVERS

There is a successful HO to the picocell if the TTT of duration T expires inside the picocell coverage area and the prediction is also inside, without touching the picocell HF circle. Once the macrocell UE has performed a successful HO to the picocell, the roles are inverted. As soon as the user leaves the picocell coverage area, it will enter the macrocell coverage area again so, if it reaches the picocell HF circle, a picocell HF is declared. We can define the distance between the picocell HF circle and the HO one as:

$$d_{\mathrm{HF,p}}(\beta, R_c, R_p) = R_c\cos(\beta) + \sqrt{R_p^2 - R_c^2\sin^2(\beta)} - d(\beta). \tag{18}$$

As in the macrocell case, we base our analysis on the distance that the user is capable of going across the TTT (24), vT. We can distinguish three cases:

1) If $vT \geq \sqrt{R_c^2 - R_f^2}$:
In this case, the UE either leaves the picocell without performing an HO or experiences an HF based on (14) and (17). Therefore, both the probability of picocell HF and PP are $\mathbb{P}_{\mathrm{HF,p}} = \mathbb{P}_{\mathrm{PP}} = 0$.
2) If $\sqrt{R_c^2 - R_f^2} < vT < 2\sqrt{R_c^2 - R_f^2}$:
In this case, in order to have a successful HO to the picocell, the chord length must be between $vT < d(\beta) < 2\sqrt{R_c^2 - R_f^2}$, i.e. $\arcsin\left(R_f/R_c\right) < \beta < \arccos\left(vT/2R\right)$. Then, a picocell HF is declared if the UE reaches the picocell HF circle before the TTT expires. From (18), we obtain:

$$vT > d_{\mathrm{HF,p}}(\beta, R_c, R_p) \Rightarrow$$
$$\beta_{\mathrm{HF,p}} < \arccos\left(\frac{R_p^2 - R_c^2 - v^2T^2}{2R_cvT}\right). \tag{19}$$

Since $\arcsin\left(R_f/R_c\right) < \beta < \beta_p$ with $\beta_p = \min\left[\left(vT/2R_c\right), \beta_{\mathrm{HF,p}}\right]$, the probability can be written as:

$$\mathbb{P}\left[l(\beta) < R_c\right] = \frac{2}{\pi}\int_{\arcsin\left(R_f/R_c\right)}^{\beta_p} 1 - Q_1\left(\frac{l(\beta)}{\sigma}, \frac{R_c}{\sigma}\right) \mathrm{d}\beta. \tag{20}$$

There is no point in using the prediction for the HO back to the macrocell because location errors could cause additional HFs. Besides, avoiding the HO to the picocell in the first place reduces the PP HOs. Ping-pong HOs happen when performing two successful consecutive HOs between the same two cells within a minimum time of stay (ToS) of duration T_{PP}. As a result, they reduce the efficiency of the network due to the frequent disconnections from the network. Note that LTE implements a hard HO. Besides, the exchange of signaling between the cells also introduces a fair amount of overhead, thus it is crucial to find a balance between the best connection available, hence the HO, and the number of unnecessary disconnections to keep a satisfactory QoS for the users. We obtain the angle β_{PP} (see Fig. 5) above which, for a given speed v, the user takes less time than T_{PP} to perform those two handovers, as:

$$2\,R_c\cos(\beta) < vT_{\mathrm{PP}} \Rightarrow \beta_{\mathrm{PP}} > \arccos\left(\frac{vT_{\mathrm{PP}}}{2R_c}\right). \tag{21}$$

Including this condition, the probability is:

$$\mathbb{P}\left[l(\beta) < R_c\right] = \frac{2}{\pi}\int_{\beta_r}^{\arccos\left(\frac{vT}{2R_c}\right)} 1 - Q_1\left(\frac{l(\beta)}{\sigma}, \frac{R_c}{\sigma}\right) \mathrm{d}\beta, \tag{22}$$

where $\beta_r = \max\left[\arcsin\left(R_f/R_c\right), \beta_{\mathrm{HF,p}}, \beta_{\mathrm{PP}}\right]$.

3) If $vT < \sqrt{R_c^2 - R_f^2}$:
In this case, even when the chord length is $d(\beta) > 2\sqrt{R_c^2 - R_f^2}$, it is possible to HO successfully to the picocell if the UE does not reach the macrocell HF circle. Then, we can divide the probability space into two. For $vT \leq d(\beta) < 2\sqrt{R_c^2 - R_f^2}$, it follows the same equation as (20), whereas for $2\sqrt{R_c^2 - R_f^2} \leq d(\beta) < 2\,R_c$, we obtain:

$$\mathbb{P}\left[l(\beta) < R_c\right] = \frac{2}{\pi}\int_{0}^{\beta_q} 1 - Q_1\left(\frac{l(\beta)}{\sigma}, \frac{R_c}{\sigma}\right) \mathrm{d}\beta, \tag{23}$$

where $\beta_q = \min\left[\arcsin\left(R_f/R_c\right), \beta_{\mathrm{HF,p}}\right]$. Combining (16) and (23), the total picocell HF probability is derived in (24), as shown at the bottom of this page.
The PP probability for this case can also be divided into two. For $vT \leq d(\beta) < 2\sqrt{R_c^2 - R_f^2}$, it is the same equation as (22), whereas for $2\sqrt{R_c^2 - R_f^2} \leq d(\beta) < 2\,R_c$, it can be expressed

$$\mathbb{P}_{\mathrm{HF,p}} = \begin{cases} 0 & \text{if } vT \geq 2\sqrt{R_c^2 - R_f^2}, \\ \mathbb{P}\left[l(\beta) < R_c\right] & \text{if } \sqrt{R_c^2 - R_f^2} < vT < 2\sqrt{R_c^2 - R_f^2}, \\ & \arcsin\left(R_f/R_c\right) < \beta \leq \arccos\left(vT/2R_c\right), \\ \mathbb{P}\left[vT < d_{\mathrm{HF,m}}(\beta, R_c, R_f)\right] \cdot \mathbb{P}\left[l(\beta) < R_c\right] + & \\ \mathbb{P}_{\mathrm{HF,p}}\Big|_{\sqrt{R_c^2 - R_f^2} < vT < 2\sqrt{R_c^2 - R_f^2}} & \text{if } vT \leq \sqrt{R_c^2 - R_f^2}, 0 < \beta \leq \arcsin\left(R_f/R_c\right). \end{cases} \tag{24}$$

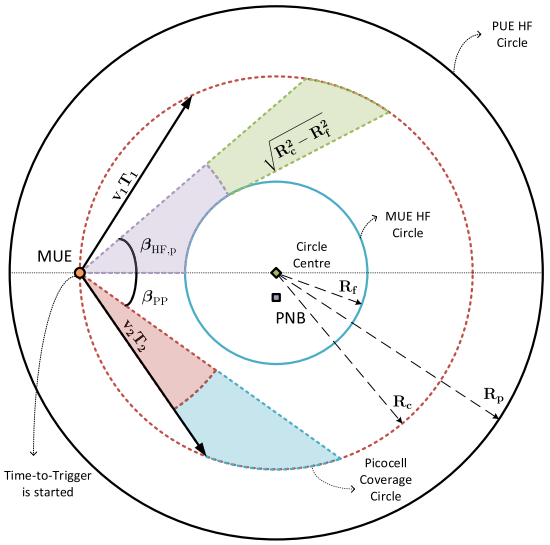

FIGURE 5. $\mathbb{P}_{\mathbf{HF,p}}$ and $\mathbb{P}_{\mathbf{PP}}$.

as (26), as shown at the bottom of this page

$$\mathbb{P}\left[l(\beta) < R_c\right] = \frac{2}{\pi} \int_{\beta_s}^{\arcsin(R_f/R_c)} 1 - Q_1\left(\frac{l(\beta)}{\sigma}, \frac{R_c}{\sigma}\right) \mathrm{d}\beta, \quad (25)$$

where $\beta_s = \max\left[0, \beta_{\mathrm{HF,p}}, \beta_{\mathrm{PP}}\right]$. The final expression is given in (26).

D. OPTIMAL PREDICTION TIMES

The utility of this analysis is providing a set of equations to choose the optimum combination of prediction times for macrocell UEs based on their speed. Different optimization problems can be proposed depending on the objective. As an example, we could define the following one:

$$\begin{aligned} &\underset{\Delta_t}{\text{minimise}}\ \mathbb{P}_{\mathrm{PP}}(\Delta_t) \\ &\text{subject to}\ \mathbb{P}_{\mathrm{HF}}(\Delta_t) \leq p_{\mathrm{out}}, \end{aligned} \quad (27)$$

where p_{out} is the outage probability, Δ_t is the timespan for the prediction, and the functions involved are derived in Sec. IV. In (27) we try to minimize the probability of ping-pong handovers allowing a certain probability of outage. We have used MATLAB to solve (27), in particular, `fmincon` (Interior Point Method).

TABLE 1. Simulation parameters.

Parameter	Value
Carrier frequency (f) [3]	2 GHz
Macrocell BS transmit power ($P_{t,m}$) [3]	46 dBm
Macro path loss model (K_m, γ_m) [35]	$128.1 + 37.6\log(R)$ dB (R in km)
Macro antenna gain (G_m) [13]	14 dBi
Picocell BS transmit power ($P_{t,p}$) [3]	30 dBm
Pico path loss model (K_p, γ_p) [35]	$140.7 + 36.7\log(R)$ dB (R in km)
Pico antenna gain (G_p) [3]	5 dBi
ISD [3]	500 m
Pico distribution radius ($r_{\max}$) [35]	289 m
Minimum distance macro-pico ($r_{\min}$) [35]	75 m
Minimum distance pico-pico [35]	40 m
Mobile UE speed (v)	10 – 120 km/h
Time-To-Trigger (T) [3]	{40, 80, 160, 480} ms
Minimum Time-of-Stay (T_{PP}) [3]	1 s
Handover Hysteresis Margin (α) [3]	0 dB
HF threshold (Q_{out}) [3]	-8 dB
Location errors std (σ) [32]	3 m
Probability of outage (p_{out})	1%
Number of simulation drops	10^7 per TTT-speed combination

V. NUMERICAL EVALUATION

In this section, we first validate the theoretical analysis derived in Section IV with Monte Carlo simulations carried out in MATLAB. We assume omnidirectional antennas at both BSs and the user and, as in the whole paper, only the path loss is considered in our analysis. Furthermore, we suppose that we have perfect knowledge of the UE RSS at any moment (geometry HO). Without loss of generality, we consider a null HHM. In case of increasing its value, the inbound HO region, macrocell to picocell, would become smaller since it is equivalent to increase the macrocell transmit power, and vice versa for the outbound HO region, picocell to macrocell, for the same reason. As depicted in Fig. 1, picocells are uniformly deployed under the coverage of a macrocell. We fix a macrocell at the origin and deploy a picocell according to (11), creating a bouncing circle around it (see green circle in Fig. 1). We have carried out 10^4 random picocell deployments. Then, we have positioned 10^3 users on the bouncing circle, connected to the macrocell at first, and make them move towards the picocell with a random angle as per 3GPP specifications [3]. For each user, the simulation ends when either an HF occurs or the UE hits the other border of the bouncing circle, whichever comes first. The results shown in the next subsections consist of the probability of no handover,

$$\mathbb{P}_{\mathrm{PP}} = \begin{cases} 0 & \text{if } vT \geq 2\sqrt{R_c^2 - R_f^2}, \\ \mathbb{P}\left[l(\beta) < R_c\right] & \text{if } \sqrt{R_c^2 - R_f^2} < vT < 2\sqrt{R_c^2 - R_f^2}, \\ & \arcsin\left(R_f/R_c\right) < \beta \leq \arccos\left(vT/2R_c\right), \\ \mathbb{P}\left[vT < d_{\mathrm{HF,m}}(\beta, R_c, R_f)\right] \cdot \mathbb{P}\left[l(\beta) < R_c\right] & \\ \quad + \mathbb{P}_{\mathrm{PP}}\Big|_{\sqrt{R_c^2 - R_f^2} < vT < 2\sqrt{R_c^2 - R_f^2}} & \text{if } vT \leq \sqrt{R_c^2 - R_f^2}, 0 < \beta \leq \arcsin\left(R_f/R_c\right). \end{cases} \quad (26)$$

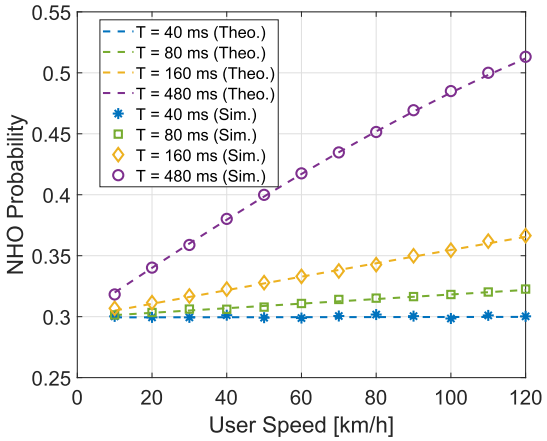

(a) Probability of no handover.

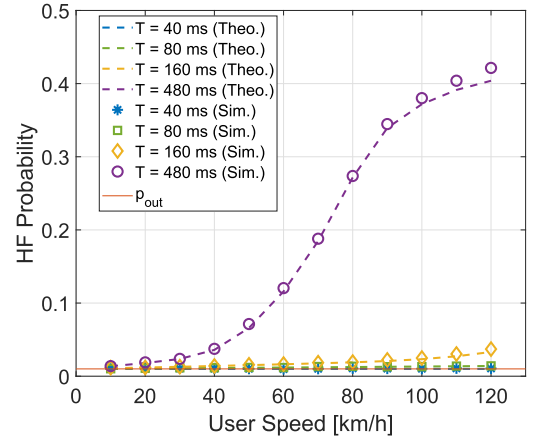

(b) Probability of handover failure.

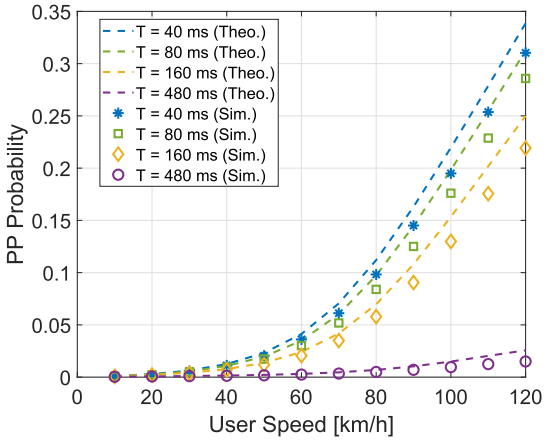

(c) Probability of ping-pong handover.

FIGURE 6. REM-HO theoretical (dashed lines) and simulated (markers) results as a function of the UE speed for TTT = {40, 80, 160, 480} ms, and Δ_t^* from (27).

the probability of handover failure (macrocell and picocell together), and the probability of ping-pong handover. Then, we compare our proposed algorithm with other algorithms found in the literature [13], [28]. Finally, we evaluate the performance of the REM-HO algorithm under the influence of different location errors. The rest of the simulation parameters are listed in Table 1.

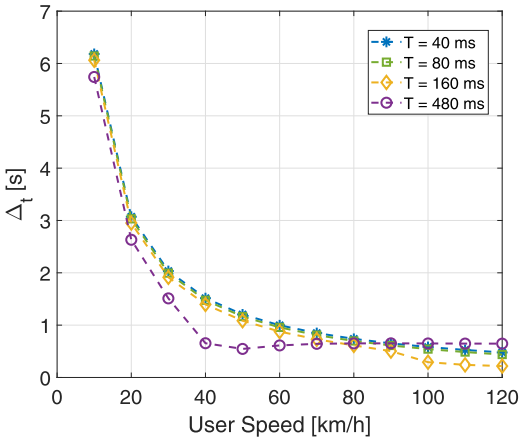

FIGURE 7. Optimal prediction times as a function of the UE speed for TTT = {40, 80, 160, 480} ms.

A. PERFORMANCE OF REM-HO

In Fig. 6, we show the theoretical and the simulation results for Δ_t^* obtained from the optimization problem in (27) versus different values of the UE speed. In general, it can be observed a good match between the theoretical values and the simulation ones. The slight differences are due to the circles in the simulation are not concentric as they are in the theoretical model. In Fig. 6a, the probability of NHO is above 30% for all speeds considered regardless of the TTT. Note that not handing over does not imply the call is dropped. It means that the UE can safely avoid the HO without an HF. The product of UE speed v and TTT T determines how much the UE travels within the picocell. Therefore, as expected, the higher this product, the more likely the UE will skip the picocell. However, this is also true for the probability of HF. In Fig. 6b, we can observe that the probability of HF is above the required $p_{out} = 1\%$ for $T = 480$ ms, i.e. the solver has been unable to find a feasible solution for (27). After 85 km/h, $T = 160$ ms rises by 1% over the limit. Only $T = 40$ ms accomplishes the target, closely followed by $T = 80$ ms at around 1.5%.

On the contrary, the probability of PP HO follows the opposite trend in Fig. 6c. In most cases, the probability of PP is within 22 – 34% for highway-speed users whereas it is less than 10% for speeds below 80 km/h. The results of the optimization problem are depicted in Fig. 7. It can be seen that the predictions are at least one order of magnitude larger than the TTTs considered, i.e. hundreds of milliseconds against tens of milliseconds, which cause the prediction times to look bundled up. The prediction time follows an inversely proportional trend to the UE speed as the longer the distance within the picocell, the higher the risk of an HF. In case we relax the constraints, we could skip HOs more aggressively while increasing the HF probability.

B. COMPARISON WITH COMPETITIVE ALGORITHMS

After validating the theoretical model, we can compare our proposed REM-HO with other competitive schemes in the same scenario. The following algorithms implemented or evaluated for the comparison are considered:

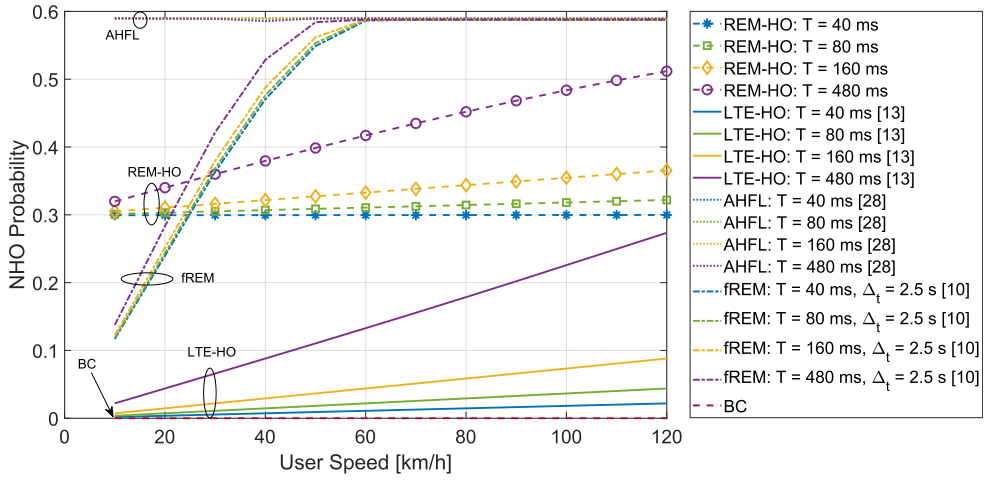

(a) Probability of no handover.

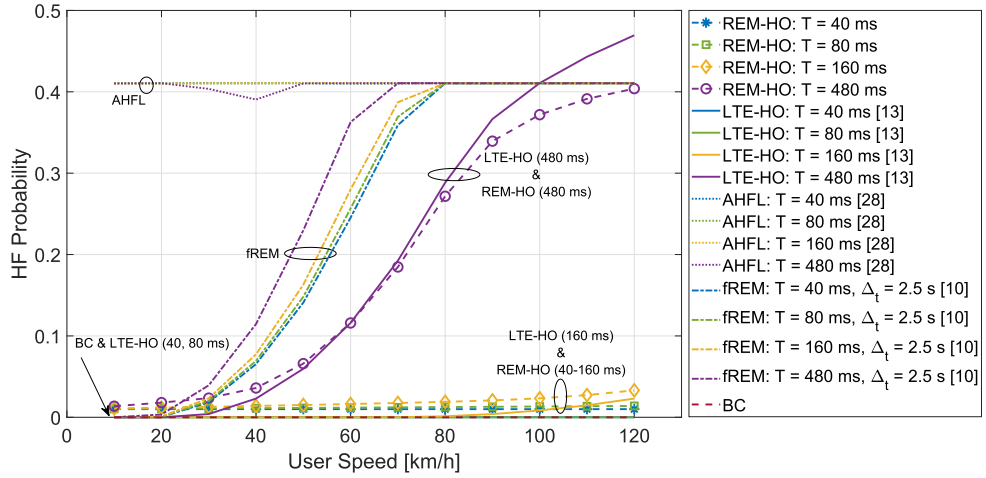

(b) Probability of handover failure.

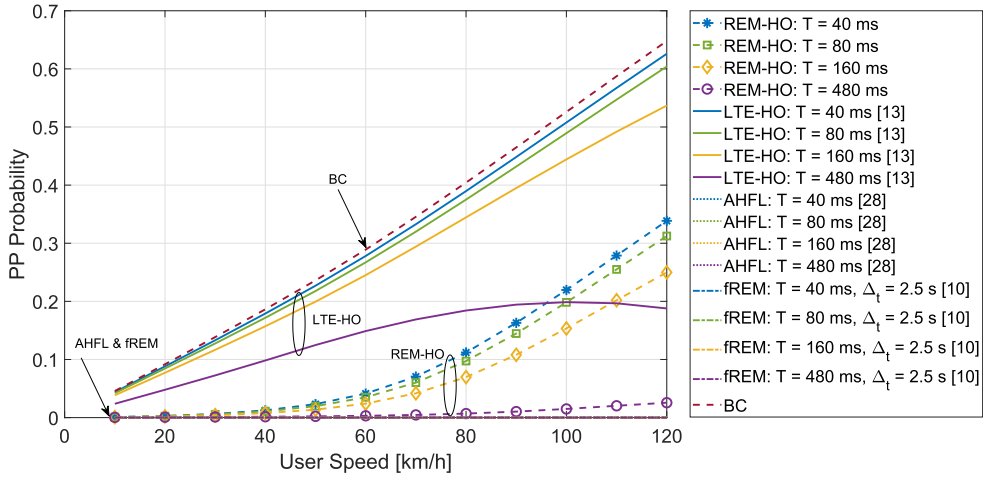

(c) Probability of ping-pong handover.

FIGURE 8. Comparison between REM-HO (dashed lines with markers), LTE-HO (solid lines), AHFL (dotted lines), fREM (dash-dot lines), and BC (dashed line without markers) results as a function of the UE speed for TTT = {40, 80, 160, 480} ms.

- Best Connected (BC): the UE always connects to the BS with the highest RSS. It is equivalent to the LTE-HO algorithm with $T = 0$ ms and $\alpha = 0$ dB.
- LTE-HO: the UE waits for the TTT to perform an HO. Without loss of generality, we consider $\alpha = 0$ dB. We have verified the analytical work

presented in [13], and have only evaluated the theoretical results.
- Adaptive HMM based on fuzzy logic (AHFL): defined in [28], it uses fuzzy logic to change the value of α.
- REM-HO with fixed prediction time (fREM): introduced in [10], the value of Δ_t could not be optimized due to the lack of analytical work. This algorithm is our previous work, and we include it to show the improvement of the new scheme.

In Fig. 8a, we can view how the probability of NHO increases for longer TTTs, as stated before. In this case, our algorithm shifts the probabilities proportionally to the product $v\Delta_t$. All REM-HO cases outperform the LTE-HO algorithm in terms of NHO. On the contrary, the BC scheme does not skip a single HO. Thus the probability of NHO stays at zero for all the speeds considered. Also, the majority of fREM cases and all the AHFL cases represent an improvement over the LTE-HO algorithm. Note that the probability of NHO implies that the UE can leave the picocell coverage area without experiencing a drop. However, the probability of HF for both schemes worsens dramatically for speeds above 20 km/h, as shown in Fig.8b. For example, the AHFL algorithm performs substantially worse than the rest of the algorithms for all the speeds. Adding up the probability of NHO and the probability of HF in the AHFL cases results in almost 1, which means that the totality of the HOs is either skipped (NHO) or dropped (HF). The fREM approach becomes as bad for speeds above 80 km/h.

On the contrary, the probability of HF is marginally higher for REM-HO in the region of low TTTs and high speed. This is because, although the TTT expires before reaching the HF macrocell circle, some predictions lie outside the picocell coverage circle, so the REM-HO method avoids the opportunity of HO. Since the UE's location is not perfect, there is always a remnant of the probability HF that our proposed algorithm cannot eliminate. In particular, the HF probability is below 1.5% throughout the considered speeds as mentioned beforehand for $T = 40 - 160$ ms. For $T = 480$ ms, the distance travelled by the UE is large enough to hit the MUE HF circle, causing an HF. This effect is depicted in Fig. 4 with the example of $v_1 T_1$. The reason why the LTE-HO algorithm performs slightly worse for high-speed users is due to the less number of avoided HOs in Fig. 8a. It would seem that the BC algorithm is a good option because it does not experience any HF. As it can be seen in Fig. 8c, it has the highest probability of PP HO due to performing all possible HOs. It is a corner case that exemplifies the trade-off between HF and PP HO.

The LTE-HO scheme reduces the probability of PP HO as the TTT increases. For values of T from 40 to 160 ms, the PP HO follows an almost linear fashion. However, for $T = 480$ ms, the PP HO reaches a plateau for speeds above 60 km/h. In this case, this trend can be explained from the higher number of HF in Fig. 8b, i.e. if there is a drop, there are fewer chances of having a PP HO. Similarly, both the AHFL and the fREM algorithms do not experience any redundant HOs because of the high number of drops. This behavior is another corner case, where these two algorithms can reduce the PP HO to zero by increasing the probability of HF. Finally, we show that for our proposed REM-HO, the probability of PP HO is significantly reduced by 10, 20, and 30% for 30, 60, and 120 km/h. Our algorithm focuses on avoiding as many HOs as possible in Fig. 8a, but without overly increasing the HF in both 40 and 80 ms cases (1%) in Fig. 8b. These results demonstrate that REMs can be successfully integrated into the HO decision process complementing the current industry standard since it is backwards compatible.

C. LOCATION-ERROR EFFECT

We want to assess the importance of the location errors, and to do so we have selected $T = \{40, 80\}$ ms because they can reduce the PP probability significantly without committing an excessive amount of HFs. Also, we sweep the location errors through σ from the 3-m case [32] to 99.9% availability at any time and location given by the 12-m case [30]. The probability of NHO depicted in Fig. 9, where the differences in performance between $\sigma = 3$ m and $\sigma = 6$ m are negligible. For $\sigma = 12$ m, we can skip more HOs at the expense of experiencing more HFs. In Fig. 9b, the probability of HF tends to be almost constant for the whole range of speeds considered. We notice that the probability of HF is 14% for $\sigma = 12$ m, which is intolerable, while it is reduced by 10% for $\sigma = 6$ m. When $\sigma = 3$ m, the performance is almost zero HF. This makes evident that our proposed technique is useful whenever the location is accurate to a certain degree, e.g. 6 m in our case. A standard GPS receiver can estimate its accuracy and forward it in the measurement reports. Thus, in case of poor conditions, our algorithm can always fall back to the standard LTE-HO by ignoring the prediction. The probability of PP is shown in Fig. 9c. We can see that the performance does not skyrocket to LTE-HO levels in any case. Note that when location errors increase, the probability of PP decreases due to the higher likelihood of experiencing an HF.

D. DISCUSSION

It is important to highlight that the location errors σ are out of our control because they are intrinsically related to the GPS device coverage. Location errors in the range of 3 m $\leq \sigma \leq$ 6 m are nearer to a realistic scenario. If we put a focus on Fig. 6b, we can spot that TTTs from 40–80 ms are the least affected by the location errors, while 160 ms could be acceptable in certain situations too. We would like to stress the importance of the prediction time Δ_t that has an essential effect on the achieved performance in the REM-HO. Note that the prediction time allows us to mitigate the impact of the PP HO in Fig. 6c, and it is fundamental to set its value accordingly to the UE speed. Overall, our proposed algorithm can achieve a low probability of HF and, at the same, to reduce the PP HOs to acceptable rates. This verifies our previous works and also manifests that breaking the LTE-HO procedure into two stages, measurements and prediction, is an excellent option to find a compromise between

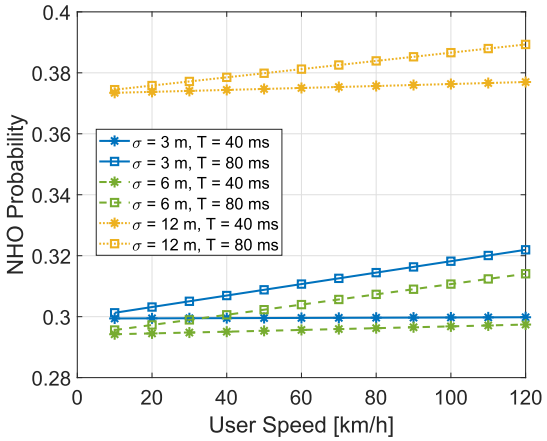

(a) Probability of no handover.

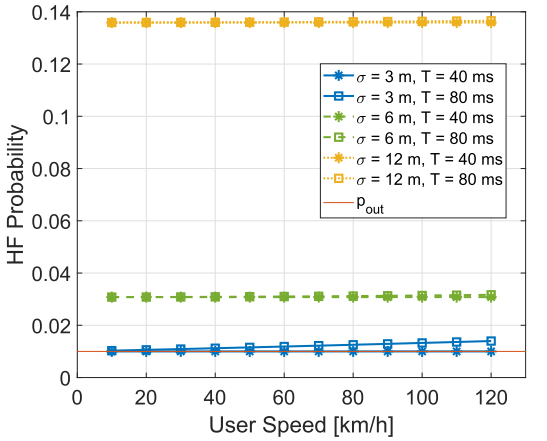

(b) Probability of handover failure.

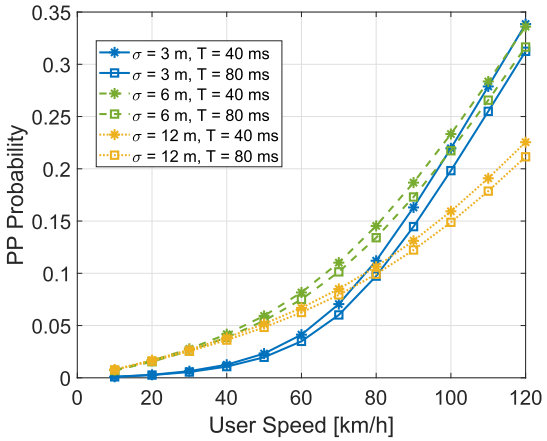

(c) Probability of ping-pong handover.

FIGURE 9. REM-HO results for TTT = {40, 80} ms, and σ = {3, 6, 12} m.

performance and backwards compatibility. Moreover, this approach is in line with the CHO approach, where we have replaced the condition for a query into a database.

VI. CONCLUSION

In this paper we have presented an HO algorithm that uses REMs as a tool to reduce the number of PP HOs without incurring too many HFs, therefore ensuring a reduction on the HetNet network signaling and future multi-tier cellular networks. Since our proposed algorithm uses the UE's geolocation capabilities, we have also derived a framework that allows us to obtain a better understanding of the expected HO performance under location errors. This framework has been validated through Monte Carlo simulations for a wide range of cases. Numerical results show that our REM-HO algorithm can drastically reduce the PP rate in most cases, maintaining it below 35%, an improvement of at least 10% over the LTE-HO standard and that the prediction time must be chosen adaptively to adjust the HF rate.

For future work, there are several incremental directions to expand the results presented in this paper. Our model already considers path loss and location errors, but it will be useful to include channel fading, in particular, shadowing, to get a more accurate framework, although the HO regions are expected not to be circles any more. Moreover, as REMs are databases, we can extract more available advanced parameters such as the load factor of each BS and perform HOs in a more proactive way (network-triggered) rather than the user-triggered network-assisted approach. To conclude, it would be interesting to tune the prediction time through an optimization problem that takes into account the HO performance obtained in this paper and the network performance as a whole.

REFERENCES

[1] Juniper Research. *White Paper: Wi-Fi Calling Operators 2017*. Accessed: May 2019. [Online]. Available: https://www.juniperresearch.com/document-library/white-papers/wi-fi-calling-operators-2017

[2] J. G. Andrews, S. Buzzi, W. Choi, S. V. Hanly, A. Lozano, A. C. K. Soong, and J. C. Zhang, "What will 5G be?" *IEEE J. Sel. Areas Commun.*, vol. 32, no. 6, pp. 1065–1082, Jun. 2014.

[3] *Evolved Universal Terrestrial Radio Access (E-UTRA); Mobility Enhancements in Heterogeneous Networks*, document 3GPP TR 36.839 V11.1.0, 2012.

[4] *Study on New Radio Access Technology; Radio Interface Protocol Aspects*, document 3GPP TR 38.804 V14.0.0, 2017.

[5] H.-S. Park, Y. Lee, T.-J. Kim, B.-C. Kim, and J.-Y. Lee, "Handover mechanism in NR for ultra-reliable low-latency communications," *IEEE Netw.*, vol. 32, no. 2, pp. 41–47, Mar./Apr. 2018.

[6] H. Martikainen, I. Viering, A. Lobinger, and T. Jokela, "On the basics of conditional handover for 5G mobility," in *Proc. IEEE 29th Annu. Int. Symp. Pers., Indoor Mobile Radio Commun. (PIMRC)*, Sep. 2018, pp. 1–7.

[7] A. Kliks, P. Kryszkiewicz, A. Umbert, J. Pérez-Romero, F. Casadevall, and L. Kulacz, "Application of radio environment maps for dynamic broadband access in TV bands in urban areas," *IEEE Access*, vol. 5, pp. 19842–19863, 2017.

[8] J. Perez-Romero, A. Zalonis, L. Boukhatem, A. Kliks, K. Koutlia, N. Dimitriou, and R. Kurda, "On the use of radio environment maps for interference management in heterogeneous networks," *IEEE Commun. Mag.*, vol. 53, no. 8, pp. 184–191, Aug. 2015.

[9] K. Sato and T. Fujii, "Kriging-based interference power constraint: Integrated design of the radio environment map and transmission power," *IEEE Trans. Cogn. Commun. Netw.*, vol. 3, no. 1, pp. 13–25, Mar. 2017.

[10] C. Suarez-Rodriguez, B. A. Jayawickrama, F. Bader, E. Dutkiewicz, and M. Heimlich, "REM-based handover algorithm for next-generation multi-tier cellular networks," in *Proc. IEEE Wireless Commun. Netw. Conf. (WCNC)*, Apr. 2018, pp. 1–6.

[11] C. Suarez-Rodriguez, B. A. Jayawickrama, Y. He, F. Bader, and M. Heimlich, "Performance analysis of REM-based handover algorithm for multi-tier cellular networks," in *Proc. IEEE 28th Annu. Int. Symp. Pers., Indoor, Mobile Radio Commun. (PIMRC)*, Oct. 2017, pp. 1–6.

[12] D. Lopez-Perez, X. Chu, and I. Guvenc, "On the expanded region of picocells in heterogeneous networks," *IEEE J. Sel. Topics Signal Process.*, vol. 6, no. 3, pp. 281–294, Jun. 2012.
[13] D. López-Pérez, I. Guvenc, and X. Chu, "Theoretical analysis of handover failure and ping-pong rates for heterogeneous networks," in *Proc. IEEE Int. Conf. Commun. (ICC)*, Jun. 2012, pp. 6774–6779.
[14] K. Vasudeva, M. Simsek, D. López-Pérez, and I. Güvenç, "Analysis of handover failures in heterogeneous networks with fading," *IEEE Trans. Veh. Technol.*, vol. 66, no. 7, pp. 6060–6074, Jul. 2017.
[15] F. Guidolin, I. Pappalardo, A. Zanella, and M. Zorzi, "Context-aware handover policies in HetNets," *IEEE Trans. Wireless Commun.*, vol. 15, no. 3, pp. 1895–1906, Mar. 2016.
[16] H. S. Dhillon, R. K. Ganti, F. Baccelli, and J. G. Andrews, "Modeling and analysis of K-tier downlink heterogeneous cellular networks," *IEEE J. Sel. Areas Commun.*, vol. 30, no. 3, pp. 550–560, Apr. 2012.
[17] H.-S. Jo, Y. J. Sang, P. Xia, and J. G. Andrews, "Heterogeneous cellular networks with flexible cell association: A comprehensive downlink SINR analysis," *IEEE Trans. Wireless Commun.*, vol. 11, no. 10, pp. 3484–3495, Oct. 2012.
[18] X. Xu, Z. Sun, X. Dai, T. Svensson, and X. Tao, "Modeling and analyzing the cross-tier handover in heterogeneous networks," *IEEE Trans. Wireless Commun.*, vol. 16, no. 12, pp. 7859–7869, Dec. 2017.
[19] W. Bao and B. Liang, "Handoff rate analysis in heterogeneous wireless networks with Poisson and Poisson cluster patterns," in *Proc. 16th ACM Int. Symp. Mobile Ad Hoc Netw. Comput. (MobiHoc)*, New York, NY, USA, 2015, pp. 77–86.
[20] W. Bao and B. Liang, "Stochastic geometric analysis of user mobility in heterogeneous wireless networks," *IEEE J. Sel. Areas Commun.*, vol. 33, no. 10, pp. 2212–2225, Oct. 2015.
[21] R. Arshad, H. ElSawy, S. Sorour, T. Y. Al-Naffouri, and M.-S. Alouini, "Velocity-aware handover management in two-tier cellular networks," *IEEE Trans. Wireless Commun.*, vol. 16, no. 3, pp. 1851–1867, Mar. 2017.
[22] R. Arshad, H. Elsawy, S. Sorour, T. Y. Al-Naffouri, and M.-S. Alouini, "Handover management in 5G and beyond: A topology aware skipping approach," *IEEE Access*, vol. 4, pp. 9073–9081, 2016.
[23] Z. Becvar and P. Mach, "Mitigation of redundant handovers to femtocells by estimation of throughput gain," *Mobile Inf. Syst.*, vol. 9, no. 4, pp. 315–330, 2013.
[24] D. Xenakis, N. Passas, L. Merakos, and C. Verikoukis, "Handover decision for small cells: Algorithms, lessons learned and simulation study," *Comput. Netw.*, vol. 100, pp. 64–74, May 2016.
[25] M.-M. Chen, Y. Yang, and Z.-D. Zhong, "Location-based handover decision algorithm in LTE networks under high-speed mobility scenario," in *Proc. IEEE 79th Veh. Technol. Conf. (VTC Spring)*, May 2014, pp. 1–5.
[26] D. Xenakis, N. Passas, L. Merakos, and C. Verikoukis, "Mobility management for femtocells in LTE-advanced: Key aspects and survey of handover decision algorithms," *IEEE Commun. Surveys Tuts.*, vol. 16, no. 1, pp. 64–91, 1st Quart., 2014.
[27] Q. Kuang, J. Belschner, Z. Bleicher, H. Droste, and J. Speidel, "A measurement-based study of handover improvement through range expansion and interference coordination," *Wireless Commun. Mobile Comput.*, vol. 15, no. 14, pp. 1784–1798, 2015.
[28] K. Da Costa Silva, Z. Becvar, and C. R. L. Frances, "Adaptive hysteresis margin based on fuzzy logic for handover in mobile networks with dense small cells," *IEEE Access*, vol. 6, pp. 17178–17189, 2018.
[29] *Radio Resource Control (RRC); Protocol Specification*, document 3GPP TR 36.331 V15.5.1, 2019.
[30] *GPS Standard Positioning Service (SPS) Performance Standard 4th Edition*, Standard GPS SPS PS, US Government, Washington, DC, USA, 2008.
[31] H. Holma, A. Toskala, and J. Reunanen, *LTE Small Cell Optimization: 3GPP Evolution to Release 13*. Hoboken, NJ, USA: Wiley, 2015.
[32] P. Ranacher, R. Brunauer, W. Trutschnig, S. Van der Spek, and S. Reich, "Why GPS makes distances bigger than they are," *Int. J. Geograph. Inf. Sci.*, vol. 30, no. 2, pp. 316–333, 2016.
[33] J. G. Proakis and M. Salehi, *Digital Communications*. New York, NY, USA: McGraw-Hill, 2007.
[34] B. A. Jayawickrama, E. Dutkiewicz, M. Mueck, and Y. He, "On the usage of geolocation-aware spectrum measurements for incumbent location and transmit power detection," *IEEE Trans. Veh. Technol.*, vol. 65, no. 10, pp. 8177–8189, Oct. 2016.
[35] *Further Advancements for E-UTRA Physical Layer Aspects*, document 3GPP TR 36.814 V9.2.0, 2017.
[36] M.-S. Alouini and A. J. Goldsmith, "Area spectral efficiency of cellular mobile radio systems," *IEEE Trans. Veh. Technol.*, vol. 48, no. 4, pp. 1047–1066, Jul. 1999.

CRISTO SUAREZ-RODRIGUEZ received the M.Sc. degree in telecommunications engineering and the M.Res. degree in intelligent systems and numeric applications in engineering from the Universidad de Las Palmas de Gran Canaria, Las Palmas, Spain, in 2013 and 2015, respectively. He is currently pursuing the Ph.D. degree with the Global Big Data Technologies Centre, University of Technology Sydney, Sydney, NSW, Australia. From 2010 to 2015, he was a Research Assistant with the Institute for Technological Development and Communication Innovation (IDeTIC), University of Las Palmas de Gran Canaria. His research interests include visible-light communications and cellular communications with an emphasis on mobility management. He was a recipient of the Accenture Award in New Services, Applications and Models of Digital Business in the 34th Spanish Official Association of Telecommunications Engineers' Awards, Madrid, Spain, in 2014.

YING HE received the B.Eng. degree in telecommunications engineering from the Beijing University of Posts and Telecommunications, China, and the Ph.D. degree in telecommunications engineering from the University of Technology Sydney, Australia, in 2009 and 2017, respectively, where she is currently a Lecturer with the School of Electrical and Data Engineering. Her research interests include physical layer algorithms in wireless communication networks, spectrum sharing, interference mitigation, and multiple radio access technologies coexistence.

ERYK DUTKIEWICZ received the B.E. degree in electrical and electronic engineering and the M.Sc. degree in applied mathematics from The University of Adelaide, in 1988 and 1992, respectively, and the Ph.D. degree in telecommunications from the University of Wollongong, in 1996. His industrial experience includes management of the Wireless Research Laboratory, Motorola, in 2000. He is currently the Head of the School of Electrical and Data Engineering, University of Technology Sydney, Australia. He is also a Professor with Hokkaido University, Japan. His current research interests include 5G and the IoT networks.